Worldwide Initiation of Holocene Marine Deltas by Deceleration of Sea-Level Rise

Daniel Jean Stanley and Andrew G. Warne

Radiocarbon-dated deltaic sequences of Holocene age from different parts of the world began to accumulate within a restricted time range, from about 8500 to 6500 years ago. Evaluation of major delta processes indicates that deceleration in sea-level rise was the key factor in Holocene delta formation. Within many deltas, there is as much as a 2000-year age range between basal deposits in seaward and landward cores. This age difference records the progressive landward migration of near mean sea-level depositional environments during the lower to mid-Holocene. Establishment of a chronostratigraphic framework for Holocene delta development provides a fundamental global baseline for distinguishing sea-level change from vertical land motion by tectonism and isostasy, and for evaluating rates of future marine incursion into low-lying deltas.

Deltas are vital food-producing areas and population centers, but as low-lying littoral regions they are highly vulnerable to even minor changes in sea level, particularly because most deltas are actively subsiding and their sediment supply has been curtailed. Moreover, predicted global warming may accelerate sea-level rise, which would intensify coastal erosion and loss of agricultural land to marine incursion (*1*). To implement long-term coastal protection measures in these sensitive areas, it is essential to understand the relation between delta development and sea-level change during the Holocene. In this report we evaluate the timing of the onset of Holocene delta formation on a worldwide basis and attempt to identify factors that were critical in inducing the accumulation of these depocenters.

The formation of modern deltas has been attributed to tectonic displacement, isostasy (vertical adjustment to sediment, glacial and water mass loading), climate, fluvial and sediment discharge, drainage basin morphology, tides, and coastal currents (*2*). Changes in sea level have also been recognized as a key factor, particularly in sequence stratigraphic studies based on seismic surveys along continental margins (*3*).

Distinguishing critical factors in the initiation of delta sequences requires a firm chronostratigraphic framework provided by radiocarbon-dated cores. Radiocarbon dating on the Mississippi delta (*4*) indicated that this depocenter began to form between 10,000 and 5000 years before the present (B.P.) (all ages in our text are in uncorrected radiocarbon years B.P.). Analysis of major modern deltas throughout the microtidal Mediterranean Sea revealed that these depocenters commenced within a period between 8000 and 6000 years B.P. (*5*). With a large number of radiocarbon-dated cores, chronostratigraphic analysis of the basal deposits in the Nile delta of northern Egypt confirmed that basal delta deposits from this region range in age from ~8000 to 6000 years B.P. (*6*, *7*).

Moreover, the Nile and other Mediterranean deltas contain a widespread and generally consistent late Pleistocene to Holocene stratigraphic succession (Fig. 1) composed of a basal sequence I of late Pleistocene fluvial deposits; an overlying sequence II of late Pleistocene to early Holocene shallow marine transgressive sandy deposits; and an upper sequence III of Holocene deltaic aggradational to progradational deposits of variable lithologies (*8*). Diastems (depositional hiatuses of brief duration) separate these three stratal units. The distinct transition from sequence II to III is readily recognizable; hence, identification and sampling of basal Holocene deltaic deposits is straightforward. Furthermore, basal sequence III deposits are generally composed of peat, lagoonal, and other organic-rich facies that accumulated at or near sea level and are amenable to radiocarbon dating (Fig. 1). It is of note that sequence III is the only deltaic portion of the late Pleistocene to Holocene section.

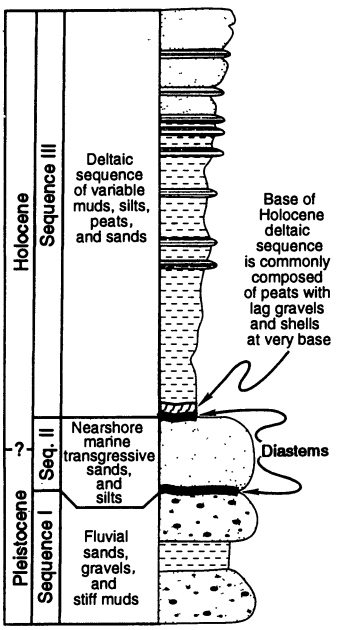

Fig. 1. Simplified lithostratigraphic section showing the threefold late Pleistocene to Holocene succession. We focused on the age of the readily identifiable base of sequence III, usually comprising near mean sea-level facies.

The consistent ~8000 to 6000 year B.P. range of basal Holocene delta deposits in these major deltas is somewhat puzzling because it is widely recognized that the interaction of geodesy, tectonics, isostasy, and eustasy has produced diverse relative sea-level histories along the Mediterranean coast (*9*). To search for common mechanisms of delta development, we compared the times of initiation of Holocene deltas in the Mediterranean with other world deltas. We surveyed the development of other deltas using a computer search of published literature (*10*). From this survey, we identified dated basal or near-basal sections in 36 Holocene deltas (Table 1 and Fig. 2) (*11*). Most dated sections are from cores, although some dates are from exposed sections particularly in those deltas undergoing glacial rebound in northern latitudes.

To get a sense of age ranges among basal delta deposits within a delta, we examined the age distribution of basal Holocene deposits across the northern Nile delta (*12*, *13*). The 64 radiocarbon-dated samples from basal Holocene sections (sequence III) of the Nile delta (Fig. 3A) are from shallow water (shoreface, lagoon, and marsh) to beach facies. These ages range from ~8500 to 5500 years B.P.: 46 (or 72%) are grouped from 8000 to 6500 years B.P., and 24 of these (or 38%) are from 7500 to 7000 years B.P. Two age populations are apparent in which the base of generally thicker Holocene core sections along the coast tend to be older than that of more landward cores (Fig. 3A). This implies that the age of basal Nile delta deposits are, in large part, determined by core location relative to distal sea and proximal apex positions. The tendency for basal Holocene delta sequences to be younger landward has also been documented in other major deltas that have been extensively cored and radiocarbon dated, such as the Rhine and Yangtze (*14*, *15*). From this information, we surmised that a variation in age of basal deposits by as much as 2000 years is to be expected within most marine deltas.

Thus, to evaluate the timing of initiation of world deltas, we selected the oldest radiocarbon age available at or near the

D. J. Stanley, Deltas-Global Change Program, Paleobiology, National Museum of Natural History, Smithsonian Institution, Washington, DC 20560, USA.
A. G. Warne, U.S. Army Corps of Engineers Waterways Experiment Station, CEWES-GG-YH Vicksburg, MS 39180, USA.

dated base of each of the 36 depocenters. The ages from basal Holocene sections of these deltas (Fig. 3B) range from ~8500 to 5500 years B.P., which is the same as for the Nile delta. Moreover, the modal age of 7500 to 7000 years B.P. for these 36 world deltas is the same as for the Nile. However, the dates for the world deltas are more skewed to older ages than for the Nile because we selected the oldest date for each of the 36 deltas (Table 1). The set of somewhat younger dates (6500 to 5500 years B.P.), accounting for 5 of 36 (or 14%) of the deltas, probably represents samples from more landward sectors of these deltas.

To determine whether climate and latitudinal position influenced delta initiation, we grouped deltas from the Mediterranean (n = 6), other mid-latitude regions (n = 18), northern (>60°) latitudes (n = 4), and tropical (between 20°S and 20°N) latitudes (n = 8) and compared their times of initiation (Fig. 3C). Deltas from these four regions cannot be differentiated as to timing of origin. Climate, isostasy, tectonism, fluvial and sediment discharge, tides, and coastal currents, among other factors, which vary considerably from region to region, could not have brought about the near-simultaneous initiation of most Holocene deltas. Therefore, we conclude that sea-level change is the only process that could induce early Holocene delta development on a worldwide basis. Sea-level change also explains the tendency for basal delta deposits to be younger in a landward direction; progressive migration landward of near mean sea-level depositional environments occurred primarily in response to rising sea level on a gently inclined surface (compare *14, 16, 17*).

In contrast to our conclusion, it has been proposed that there is no worldwide sea-level curve and each region has its own sea-level history (*9, 18*). However, certain general late Quaternary sea-level patterns are widely recognized. Compilations of world sea-level data based on radiocarbon dates from both submergent and emergent coastlines show that sea level rose rapidly between ~18,000 and 10,000 years B.P., with a notable decrease at ~11,000 years B.P. (*19*). Rates of sea-level rise decelerated during the period from 10,000 to 6000 years B.P. (*20*), and sea level approached its present stand by ~5000 years B.P. (*9*). Sea-level histories from different parts of the world differ substantially for the period ~6000 to 2000 radiocarbon years B.P. (*18*). Comparison of sea-level histories from diverse latitudinal, climatic, and isostatic and tectonic settings reveals that nearly all sea-level curves converge at ~7000 radiocarbon years during a period of deceleration in sea-level rise (*21*), perhaps indicating a worldwide geoidal eustatic response at ~8000 to 7000 years B.P. (Fig. 3D).

We conclude that deceleration in sea-level rise was the key to initiation of deltas between ~8500 and 6500 years B.P., and that Holocene deltaic sequences began to accumulate as the rate of fluvial sediment input overtook the declining rate of sea-level rise along coasts. As determined by radiocarbon data, this threshold occurred on a worldwide basis within a timespan of ~2000 years.

Establishing the direct relation between initiation of Holocene deltas and deceleration of sea-level rise provides a chronostratigraphic baseline. With this time-stratigraphic marker, it is possible to more

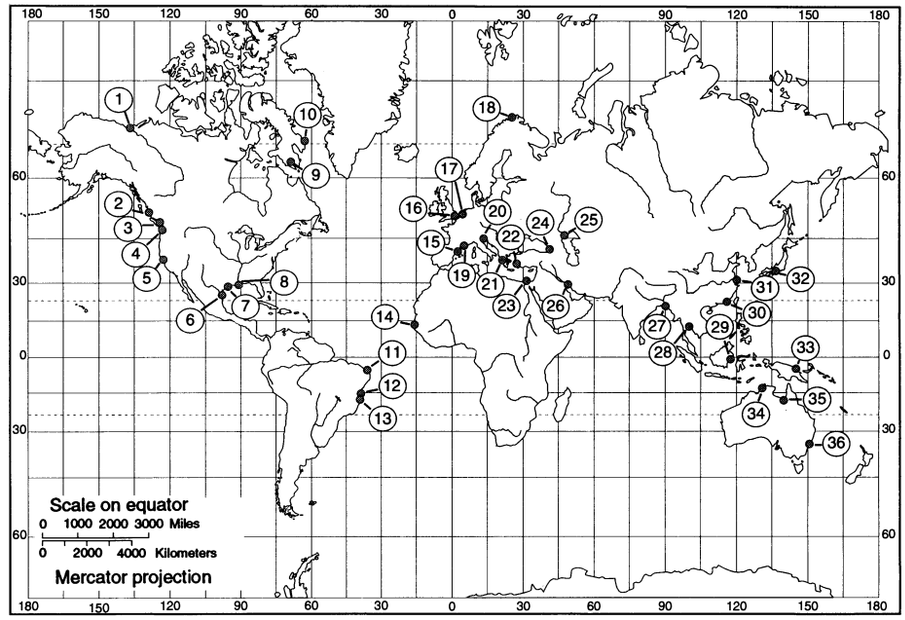

Fig. 2. Map showing positions of the 36 Holocene deltas examined in this study. Pertinent information regarding deltas is summarized in Table 1 and in (*11*).

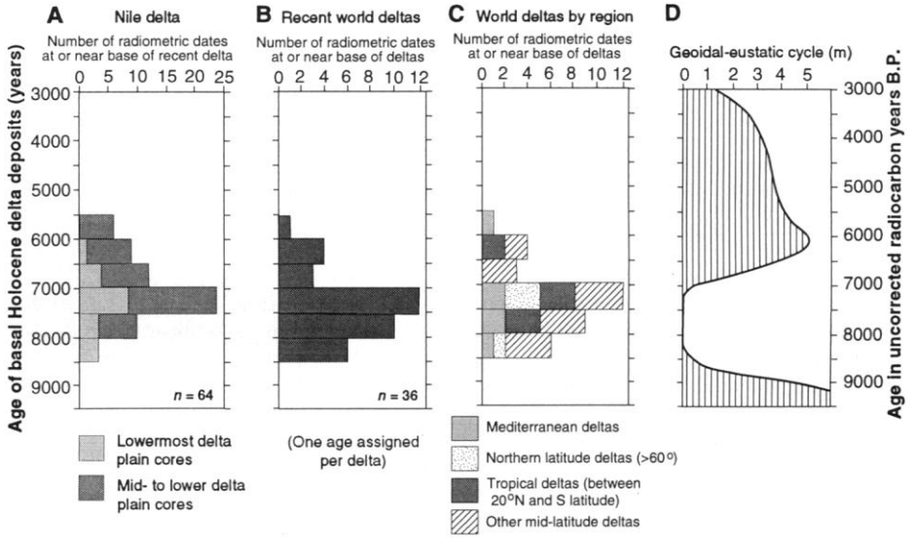

Fig. 3. Summary of age data from the 36 Holocene deltas. (**A**) Age distribution of basal Nile delta deposits, differentiating dates from 19 samples collected in lowermost delta plain cores from 45 samples collected in landward, mid- to lower delta plain cores. (**B**) Age distribution of oldest dated basal Holocene sections from the 36 deltas considered in this study (Table 1); delta positions are shown in Fig. 2. (**C**) Age distribution of basal Holocene sections from the 36 deltas, depicted by geographic position. (**D**) Geoidal-eustatic cycle, as related to core-mantle changes [modified after (*21*)], showing a marked change during the 8000 to 7000 year B.P. period, which closely corresponds with initiation of most world deltas examined in this report. Curve converted from sidereal to radiocarbon years B.P. [compare with (*21*)].

Table 1. Listing of oldest published dates (in radiocarbon years B.P.) in basal sections of Holocene deltas considered in this report. Dates preceded by ">" symbol record ages from above the very base of delta section. Delta positions, as indicated by the code in the first column, are shown in Fig. 2; reference sources, denoted by the same code, are listed in (*11*).

Code	Delta	Country	Age of (near) basal Holocene (years)
1	McKenzie	Canada	>6900 ± 110
2	British Columbia Fjord-Head Deltas	Canada	~8500
3a	Fraser	Canada	7300 ± 130
3b	Fraser	Canada	7960 ± 140
3c	Fraser	Canada	7650 ± 140
4	Snohomish	USA	~7000
5	Sacramento–San Joaquin	USA	6805 ± 650
6	Rio Grande	USA	~7000
7	Central Texas Coast Deltas	USA	>6670 ± 100
8a	Mississippi	USA	7240 ± 160
8b	Mississippi	USA	7880 ± 520
8c	Mississippi	USA	~6800
9	Baffin Island (SW)	Canada	7285 ± 200
10	Baffin Island (SE)	Canada	7100 ± 140
11	Acu	Brazil	>7020 ± 100
12	Jequitinhonha	Brazil	7900
13	Doce	Brazil	~7000
14	Saloum	Senegal	>6130 ± 130
15	Ebro	Spain	7680 ± 350
16	Thames Floodplain	England	7830 ± 110
17a	Rhine	Netherlands	8000
17b	Rhine	Netherlands	7420 ± 150
18	Alta	Norway	~7000
19a	Rhone	France	7860 ± 110
19b	Rhone	France	7200
20	Po	Italy	~7000
21	Acheloos	Greece	>5720
22	Gediz	Turkey	>7150 ± 110
23	Nile	Egypt	8140 ± 130
24	Poti	Russia	7900 ± 60
25	Volga	Russia	~8500
26a	Tigris-Euphrates	Kuwait	5980
26b	Tigris-Euphrates	Kuwait	8490 ± 100
27	Ganges	Bengladesh	7060 ± 120
28	Chao Phraya	Thailand	7800 ± 40
29	Mahakam	Borneo	~7500
30	Han	China	>6320 ± 240
31a	Yangtze	China	8320 ± 170
31b	Yangtze	China	7370 ± 140
32	Nobi	Japan	~6300
33	Sepik-Ramu	Papua, New Guinea	>7130 ± 250
34	Daly	Australia	7540 ± 110
35	Gilbert	Australia	>6430 ± 120
36	Georges	Australia	~7000

accurately distinguish and measure the influence of other major delta processes, such as tectonic displacement and isostasy, which have induced vertical land motion and thus have influenced delta plain development. For example, such a baseline has already proven invaluable in evaluating long-term subsidence rates, the effects of neotectonism, and the rate of wetland loss in the Nile delta (*7*, *22*). The 8500 to 6500 years B.P. baseline can also be used as a long-term standard to augment shorter term (century or less) tide-gauge data (compare *23*). This information is essential for planning and implementing effective shoreline protection measures needed for low-lying deltas prone to marine incursion. As human population levels in coastal deltas continue to escalate, and as dependency on agricultural production from these fertile regions continues to increase (*24*), more precise definition of the relation between sea-level change and delta evolution is critical.

REFERENCES AND NOTES

1. R. J. N. Devoy, Ed., *Sea Surface Studies: A Global View* (Croom Helm, London, 1987); J. D. Milliman, J. M. Broadus, F. Gable, *Ambio* **18**, 340 (1989); L. Jeftic, J. D. Milliman, G. Sestini, Eds., *Climate Change and the Mediterranean* (Arnold, New York, 1992).
2. J. M. Coleman, *Deltas: Processes of Deposition and Models for Exploration* (International Human Resources Development Corporation, Boston, ed. 2, 1982); W. E. Galloway and D. K. Hobday, *Terrigenous Clastic Depositional Systems: Applications to Petroleum, Coal, and Uranium Exploration* (Springer, New York, 1983); A. Colella and D. B. Prior, Eds., *Coarse-Grained Deltas* (Blackwell, Boston, 1990).
3. J. R. Suter and H. L. Berryhill Jr., *Am. Assoc. Petrol. Geol. Bull.* **69**, 77 (1985); M. Tesson, B. Gensous, G. L. Allen, Ch. Ravenne, *Mar. Geol.* **91**, 325 (1990).
4. H. N. Fisk and E. McFarlan Jr., *Geol. Soc. Am. Spec. Pap.* **62**, 279 (1955).
5. D. J. Stanley, *Int. Geol. Congr. Abstr.* **3**, 1 (1989).
6. ———, *Mar. Geol.* **94**, 147 (1990).
7. ——— and A. G. Warne, *Science* **260**, 628 (1993).
8. ———, *Nature* **363**, 435 (1993).
9. P. A. Pirazzoli, *World Atlas of Holocene Sea-Level Changes* (Elsevier, Amsterdam, 1991).
10. We devised a library computer search strategy, using the GeoRef database, by means of the EPIC System. We used the following GeoRef Thesaurus search terms: delta, deltaic, Holocene, late Quaternary, radiocarbon dating, C-14, and carbon-14. The on-line search was supplemented by an in-depth review of reference lists from delta literature and by consultation with colleagues researching different world deltas. This search provided approximately 350 journal and book articles, of which 45 provided clearly identifiable dated basal or near-basal sections from 36 Holocene deltas.
11. The following are source references for radiocarbon dates available for basal sections of the 36 world deltas that we considered and depicted in Fig. 2; numbers in parentheses and letter codes refer to those listed in column 1 of Table 1. (1) G. H. Johnston and R. J. E. Brown, *Geol. Soc. Am. Bull.* **76**, 103 (1965). (2) D. B. Prior and B. D. Bornhold, in *Coarse-Grained Deltas*, A. Colella and D. B. Prior, Eds. (Blackwell, Boston, 1990), pp. 75–90. (3a) W. H. Matthews and F. P. Shepard, *Am. Ass. Petrol. Geol. Bull.* **46**, 1416 (1962); (3b) H. F. L. Williams and M. C. Roberts, *Can. J. Earth Sci.* **26**, 1657 (1989); (3c) R. McNeely and P. K. Jorgensen, *Geol. Surv. Can. Pap.* **91-7**, 41 (1993). (4) S. R. Fuller, J. N. Sondergaard, P. F. Fuglevand, *Wash. Div. Geol. Earth Resour. Bull.* **78**, 1165 (1989). (5) B. F. Atwater, thesis, University of Delaware, Newark (1980). (6) W. A. Pryor and K. Fulton, in *Fifth Symposium on Improved Methods for Oil Recovery Proceedings*, Society of Petroleum Engineers, American Institute of Mining Engineers (AIME), Tulsa, OK, 16 to 19 April 1978 (Society of Petroleum Engineers, AIME, Tulsa, 1978), pp. 81–96. (7) B. H. Wilkinson and R. A. Basse, *Geol. Soc. Am. Bull.* **89**, 1592 (1978). (8a) J. M. Coleman and W. G. Smith, *ibid.* **75**, 833 (1964); (8b) reference (*16*); (8c) S. Penland, R. A. McBride, S. J. Williams, R. Boyd, J. R. Suter, in *Coastal Sediments 1991 Volume II*, N. C. Kraus, K. J. Gingerich, D. L. Kriebel, Eds. (American Society of Civil Engineers, New York, 1991), pp. 1248–1264; and reference (*16*). (9) J. D. Jacobs, W. N. Mode, C. A. Squires, G. H. Miller, *Geogr. Phys. Quaternaire* **39**, 151 (1985). (10) G. H. Miller, *Quat. Res.* **3**, 561 (1973). (11) C. G. Silva, thesis, Duke University, Durham, NC (1991). (12) J. M. L. Dominguez, L. Martin, A. C. Bittencourt, *Soc. Econ. Paleontol. Mineral. Spec. Publ.* **41**, 127 (1987). (13) K. Suguio and L. Martin, *Geo-Mar. Lett.* **1**, 181 (1981). (14) J. Ausseil-Badie *et al.*, *Quat. Res.* **36**, 178 (1991). (15) A. Maldonado, in *Deltas Models for Exploration*, M. L. Broussard, Ed. (Houston Geological Society, Houston, TX, 1975), pp. 311–338. (16) R. J. N. Devoy, *Philos. Trans. R. Soc. London* **285** (1010), 355 (1979). (17) reference (*13*). (18) G. D. Corner, E. Nordahl, K. Munch-Ellingsen, K. R. Robertsen, in *Coarse-Grained Deltas*, A. Colella and D. B. Prior, Eds. (Blackwell, Boston, 1990), pp. 155–168. (19a) J.-C. Aloisi, A. Monaco, J. Thommeret, Y. Thommeret, *Rev. Géogr. Phys. Géol. Dyn.* **17**, 13 (1975); (19b) A. L'Homer, F. Brazile, J. Thommeret, Y. Thommeret, *Oceanis* **7**, 38 (1981). (20) G. Sestini, in *Climatic Change and the Mediterranean*, L. Jeftic, J. D. Milliman, G. Sestini, Eds. (Arnold, New York, 1992), pp. 458–494. (21) C. A. Villas, thesis, University of Delaware, Newark,

(1984). (22) A. E. Asku and D. J. W. Piper, *Mar. Geol.* **54**, 1 (1984). (23) reference (*6*). (24) L. I. Bogolyubova, *Lithol. Miner. Resour.* **25**, 54 (1990). (25) Y. F. Belevich, *Izv. Akad. Nauk SSSR Ser. Geograf.* **1987**, 82 (1987). (26a) P. Kassler, in *The Persian Gulf*, B. H. Purser, Ed. (Springer, New York, 1973), pp. 11–32; (26b) P. Sanlaville, *Paléorient* **15**, 5 (1989). (27) M. Umitsu, *Sediment. Geol.* **83**, 177 (1993). (28) J. R. P. Somboon and N. Thiramongkol, *J. S. E. Asian Earth Sci.* **7**, 53 (1992). (29) G. P. Allen, D. Laurier, J. P. Thouvenin, *TOTAL, Cie. Fr. Pet., Notes Mém.* **15**, 1 (1979). (30) Y. Zong, *J. Coastal Res.* **8**, 1 (1992). (31a) K.-B. Liu, S. Sun, X. Jiang, *Quat. Res.* **38**, 32 (1992); (31b) reference (*14*). (32) S. Mori, *J. Earth Sci. Nagoya Univ.* **34**, 109 (1986). (33) J. Chappell, *Sediment. Geol.* **83**, 339 (1993). (34) *ibid.*, p. 339; (35) B. G. Jones, G. R. Martin, N. Senapati, *ibid.*, p. 319. (36) P. S. Roy and E. A. Crawford, *Rec. Geol. Surv. N.S.W.* **20**, 160 (1981).

12. MEDIBA (Mediterranean Basin Program), *Nile Delta Project Database Listings*, (U.S. National Museum of Natural History Records, Washington, DC, 1994).
13. Analysis is based on more than 4000 petrographic samples from 87 long drill cores [positions shown in (*7*)]. Almost all cores have been radiocarbon dated (total of ~400 dates), of which 64 dates were obtained from samples at or near the base of Holocene deltaic sequence III (Fig. 1).
14. T. E. Törnqvist, *J. Sediment. Petrol.* **63**, 683 (1993); *Fluvial Sedimentary Geology and Chronology of the Holocene Rhine-Meuse Delta, The Netherlands* (Faculteit Ruimtelijke, Utrecht, The Netherlands, 1993).
15. D. J. Stanley and Z. Chen, *Mar. Geol.* **112**, 1 (1993).
16. P. C. Scruton, in *Recent Sediments, Northwest Gulf of Mexico*, F. P. Shepard, F. P. Phleger, Tj. H. van Andel, Eds. (American Association of Petroleum Geologists, Tulsa, OK, 1960), pp. 82–102.
17. D. E. Frazier, *Tex. Bur. Econ. Geol. Geol. Circ. 74-1* (1974).
18. O. van de Plassche, Ed., *Sea-Level Research: A Manual for the Collection and Evaluation of Data* (Geo Books, Norwich, England, 1986); D. B. Scott, P. A. Pirazzoli, C. A. Honig, Eds., *Late Quaternary Sea-Level Correlation and Applications* (Kluwer Academic, Boston, 1989).
19. R. G. Fairbanks, *Nature* **342**, 637 (1989).
20. R. G. Lighty, I. G. Macintyre, R. Stuckenrath, *Coral Reefs* **1**, 125 (1982); W. S. Newman, R. R. Pardi, R. W. Fairbridge, in *Late Quaternary Sea-Level Correlation and Applications*, D. B. Scott, P. A. Pirazzoli, C. A. Honig, Eds. (Kluwer Academic, Boston, 1989), pp. 207–228.
21. N.-A. Mörner, in *Earth Rheology, Isotasy and Eustasy*, N.-A. Mörner, Ed. (Wiley, New York, 1980), pp. 535–553.
22. A. G. Warne and D. J. Stanley, *Geology* **21**, 715 (1993).
23. K. O. Emery and D. G. Aubrey, *Sea Levels, Land Levels and Tide Gauges* (Springer, New York, 1991).
24. S. Postel, *Last Oasis: Facing Water Scarcity* (Norton, New York, 1992); International Bank for Reconstruction and Development–World Bank, *World Population Projections* (John Hopkins Univ. Press, Baltimore, 1993); C. Rosenzweig and M. L. Perry, *Nature* **367**, 133 (1994).
25. We thank W. Autin, Z. Chen, I. G. Macintyre, W. A. DiMichele, R. T. Saucier, T. E. Törnqvist, J. Schneiderman, L. M. Smith, W. Pizzolato, M. K. Corcoran, and D. T. Steere Jr. for their assistance, advice, and reviews. Funding was provided by Smithsonian Scholarly Studies Program and National Geographic Society grants.

22 February 1994; accepted 13 May 1994

"Molecule Corrals" for Studies of Monolayer Organic Films

David L. Patrick, Victor J. Cee, Thomas P. Beebe Jr.*

Scanning tunneling microscopy (STM) studies have demonstrated that monolayer-deep, flat-bottomed, circular etch pits can be grown on highly ordered pyrolytic graphite by high-temperature etching in the presence of oxygen. In this work, these graphite etch pits are used as "molecule corrals" to isolate ensembles of molecules for study by STM. The nucleation of self-assembled molecular films in the corrals took place by nucleation events separate from those leading to self-assembly on the surrounding terrace and allowed the measurement of the nucleation rate constant in the corrals. The dependence of the nucleation rate for self-assembly on pit size shows that nucleation occurs at open terrace sites and that step edges (that is, the corral's perimeter) and confinement inhibit film growth.

Molecular self-assembly of organic thin films on solid surfaces has long been an area of interest in fields ranging from materials science to biology (*1*). Self-assembled films, in addition to exhibiting a rich variety of scientifically interesting properties, are promising candidates for use in a number of applications, from chemical sensors to nonlinear optical devices (*2*). In this report, we describe an investigation of self-assembled liquid crystal films on graphite designed to study (i) nucleation and growth processes in thin molecular films and (ii) the degree of interaction between molecules in adjacent molecular domains. A new approach, in which nanometer-sized "molecule corrals" are used to confine molecule ensembles within small regions, permits the analysis of molecular behavior by statistical methods and allows the measurement of several important properties difficult or impossible to determine by other techniques. We show that etch pits offer a practical method for confining molecules to small surface regions and allow the observation of multiple independent sample domains with STM. Other researchers have built corrals atom by atom at 4 K to study the properties of confined wave functions (*3*); we use corrals to study the behavior of molecules on surfaces. The ease with which these corrals can be constructed using standard laboratory apparatus makes them appealing for use in a wide range of studies.

The construction of molecule corrals is based on a chemical modification of highly oriented pyrolytic graphite (HOPG) that occurs when it is heated in the presence of O_2 at ~650°C (*4*). Carbon removal by oxidation around preexisting point defects results in the creation of monolayer-deep, flat-bottomed etch pits with surface densities from 1 to 25 μm^{-2} (*5*, *6*). Circular etch pits with diameters between 50 and 5000 Å are readily formed, and their size can be accurately controlled by varying the heating temperature and time. Noncircular, irregularly shaped etch pits can also be made by repeated heating at 1000°C in air for short (~15 s) intervals.

The molecule used, 4′-octyl-4-biphenylcarbonitrile (8CB), was chosen because many of its bulk and surface properties are known from previous studies (*7*), although preliminary experiments on other systems indicate that the use of molecule corrals is not limited to this molecule. We applied 8CB directly to etched HOPG surfaces as a neat liquid, in air at a slightly warm room temperature of 26° ± 1°C. At this temperature, 8CB is a bulk smectic-A phase with a thick, honey-like consistency. Each HOPG sample was covered with a macroscopic thickness of 8CB. The STM tip plunges through all intervening layers to image only the molecules directly adsorbed to the substrate (*7*).

The STM image in Fig. 1A shows three corrals, two of which are 800 Å in diameter and one that is 1400 Å in diameter, on an HOPG surface covered with a film of 8CB. The closely spaced (38 ± 1 Å) lines on the terrace and in two of the monolayer-deep corrals are parallel rows of self-assembled molecules adsorbed to the HOPG surface (*8*). The row structure in a low-resolution image like Fig. 1A arises from the molecular details of the unit cell, which are resolved in Fig. 1B, with an interrow spacing equal to $\beta\cos(90-\theta)$, where β and θ are defined as in Fig. 1B. The image in Fig. 1A was taken several hours after the film was applied, and self-assembled monolayers had formed in two of the three corrals. The third corral, which appears empty, was likely filled with molecules in a disordered state [which cannot be imaged by STM because of the relative time scales of their thermal motion and image acquisition (*9*)].

Department of Chemistry, University of Utah, Salt Lake City, UT 84112, USA.

*To whom correspondence should be addressed.